



Report on Sapphire Suspension Modelling and Strength Testing

ET-0009A-14

Giles Hammond, Rebecca Douglas, Alan Cumming, Sheena Barclay, Sheila Rowan

Institute for Gravitational Research, University of Glasgow

on behalf of ELITES WP1 and WP2

1. Introduction

Modelling and experiments have been carried out by researchers at the Institute for Gravitational Research to investigate and prove the feasibility of sapphire suspension elements for the KAGRA detector. During year 2 of the ELiTES project: (i) we have performed modelling to assess the thermal noise performance of sapphire springs at the intermediate mass, and their effect on the resonant modes of the suspension (ii) built a custom strength tester to analyse the breaking strength of sapphire plates with mechanically polished and thermo-polished surfaces (iii) performed static and dynamic strength tests on sapphire fibres produced by IMPEX with both monolithic and brazed ends.

2. Thermal Noise Modelling of the Final Stage

Modelling has been performed to assess the effect of adding cantilever springs onto the final monolithic stage of the KAGRA cryogenic payload in an attempt to lower the vertical bounce frequency and provide additional compliance to take account of variation in fibre length. The KAGRA cryogenic payload has been modelled using the aLIGO Mathematica model written by Mark Barton [1]. A number of modifications have been added to facilitate modelling the KAGRA design.

- model a payload comprising an intermediate mass which supports a recoil mass and test mass. The intermediate mass is coupled to the support (platform) via a cantilever spring.
- incorporate cantilever springs with vertical compliance into the final test mass stage
- model the suspension at a temperature of 20 K and assuming the following materials

Upper springs: maraging steel, upper wire: maraging steel, intermediate mass: copper with a mass 60.9 kg, recoil wire: tungsten, recoil mass: copper with a mass 37.2kg, test mass fibre: sapphire, test mass: sapphire with a mass 23 kg, operating temperature: 20 K

Figure 1 shows a schematic of the modelled system (a) with no springs at the final stage (b) with springs at the final stage. The springs are denoted by the small cubes.

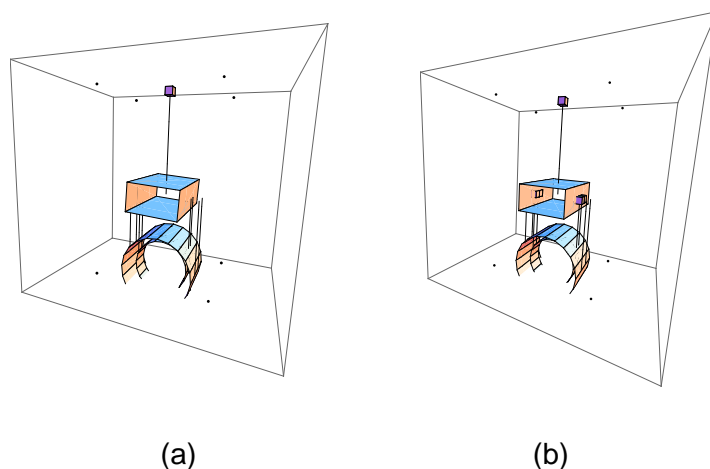


Figure 1. (a) Mathematica model configuration without final stage springs (b) Mathematica model configuration with final stage springs

The thermo-mechanical and damping parameters for the different suspension components were estimated from both measurements presented in the literature and private communication [2]. The values in Appendix A (table A1) were used as an initial estimate (these should be revised whenever new measurements are available). The parameters critical for the estimation of the thermal noise are the bulk damping of the metal wires/springs (where a value of 10^{-4} is assumed) and the surface loss of the sapphire fibres (currently being measured). The model assumes surface loss and bulk loss in the components as well as thermoelastic loss.

2.1 Spring Sizing

The upper mass is assumed to be suspended from a spring with an uncoupled vertical frequency of 3 Hz. This choice has little effect to the thermal noise performance but does assume that the stiffness is

$$k_U = \sqrt{4\pi^2 m_1 f^2} \approx 21 \text{ kN} / \text{m}$$

where it is assumed that a single wire supports the mass $m_1=60.9\text{kg}$. For the final stage springs with an uncoupled resonance frequency of 20 Hz we find

$$k_L = \sqrt{4\pi^2 \left(\frac{m_2}{4}\right) f^2} \approx 90 \text{ kN} / \text{m}$$

where 4 wires suspend the $m_2=23$ kg optic. This spring will deflect approximately 0.6 mm under the nominal load. This is significantly more than the $20 \mu\text{m}$ stretch of the sapphire fibres and this will ease the challenges associated with matching the tension on each of the fibres. The springs are sized according to their Young's modulus (Y), base width (w) and length (L) via

$$t_U = \sqrt[3]{\frac{6L^3 k_U}{w_U Y_U}}$$

which results in a thickness 5mm for the upper springs. This thickness defines the characteristic peak frequency of the thermoelastic damping. A similar expression is used to model springs supporting the optic where a choice of either maraging steel or sapphire is assumed.

2.2 Thermal Noise without Springs

The case of no springs supporting the final stage results in a suspension with the highest vertical and roll frequencies. Previous finite element estimates have given these frequencies at 108 Hz and 166 Hz. However this always assumed that the intermediate mass was rigidly fixed. In reality the modal frequencies are somewhat higher (a factor of $\sqrt{2}$ if both the optic and the intermediate mass were identical) at 145 Hz and 195 Hz. It is further assumed in this model that all wire attachments are at the centre of mass of the optic, and that the bending occurs either above/below the mass according to the wire tension and wire geometry (e.g. the flex point of the wire). These assumptions can be further refined as the suspension design is finalised.

The thermal noise contribution due to the pendulum motion and 0.3% (set by the KAGRA tunnel geometry) vertical motion is shown in figure 2 for the KAGRA baseline (taken from the requirement strain curve) and the total thermal noise contribution without springs.

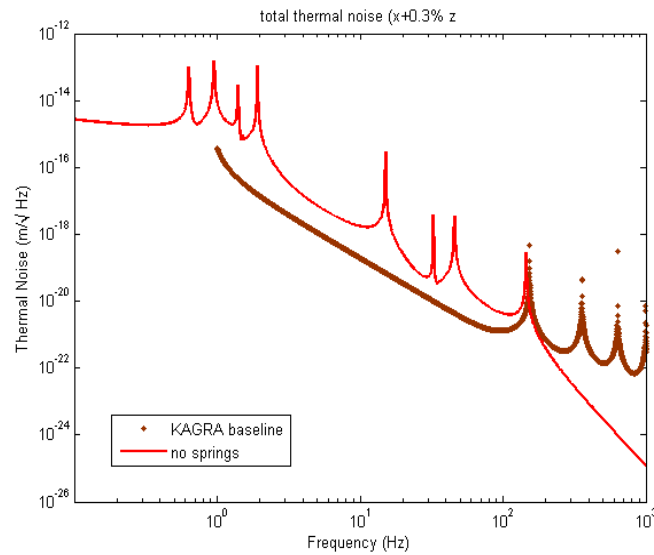


Figure 2. Thermal noise estimate without springs at the final stage (for a single test mass)

To further investigate the dominant noise contribution the different loss terms for the recoil mass wires and test mass fibres were set to zero individually. Figure 3 shows the following cases; red line: all losses included, green dots: reaction wire loss set to zero, blue dots: fibre loss set to zero. As can be seen from this figure the dominant noise contribution arises from the recoil mass wires and thus it is important to further verify the mechanical loss of the Tungsten wires at low temperature (a value of 10^{-4} is assumed here).

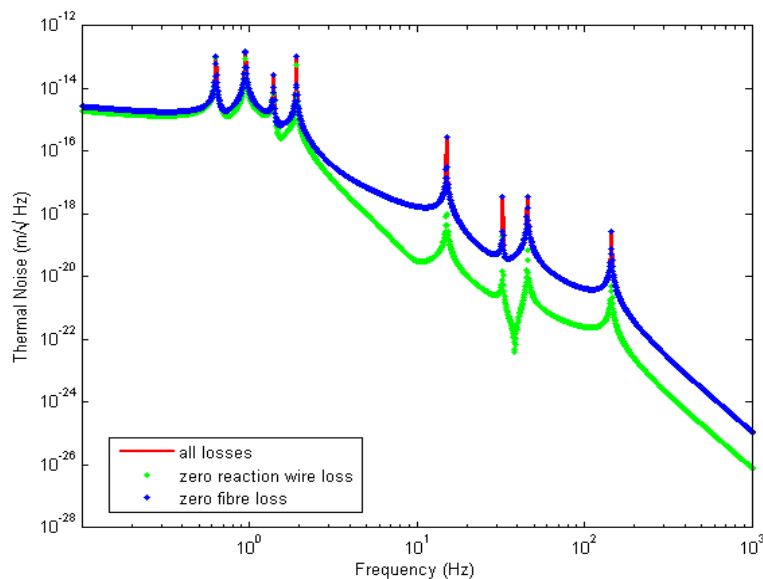


Figure 3. Thermal noise estimate without springs and for the different loss terms set to zero

The dominant coupling above 30 Hz arises from the 0.3% vertical component of thermal noise as shown in figure 4. This is presumably as a result of the high vertical stiffness of the sapphire fibres used in the final stage of the test mass suspension.

2.3 Springs at the Final Stage

The option of maraging steel and sapphire springs at the final stage was modelled in order to assess the thermal noise implications. A conservative uncoupled frequency of 20 Hz was assumed which allowed springs to operate at stress level around 20-40 MPa. A significantly lower stiffness does not reduce the eigenfrequencies of the suspension much below 50-60 Hz, although a softer spring would benefit in the static vertical suspension alignment.

Figure 5 shows the thermal noise for the two spring varieties, in addition to the loss predicted from section 2.2 (e.g. no springs). The cases considered are; brown dots: KAGRA baseline taken from the requirement strain curve and turned into the thermal noise for a single mass (e.g. multiplying by 3000/2), red line: no springs at the intermediate mass, magenta line: 20 Hz maraging steel springs supporting the optic, black line: 20Hz sapphire springs supporting the optic.

The benefit of the springs is clear from the modal point of view with the highest vertical mode below 50 Hz. The maraging steel springs do have a worse thermal noise performance above 250 Hz than the model without springs, but this is still below the KAGRA baseline at these higher frequencies. The sapphire springs give significant benefit over both of the other cases and meet the KAGRA requirements down to the body mode frequencies of the suspension.

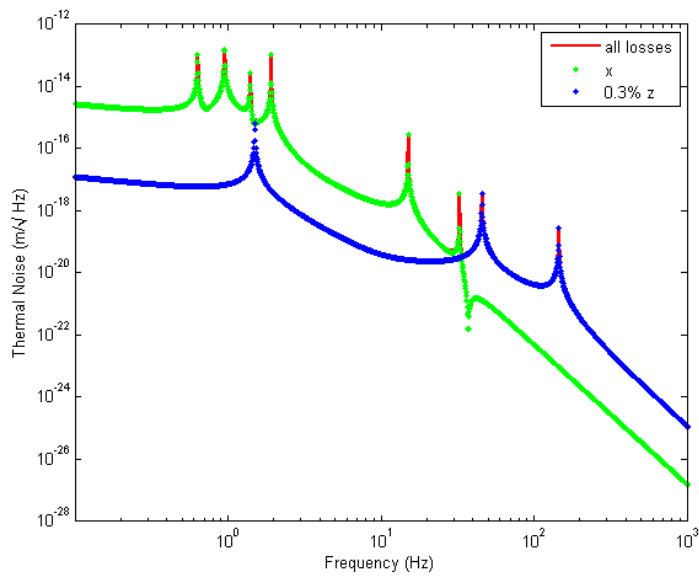


Figure 4. Thermal noise contribution from the recoil mass wires

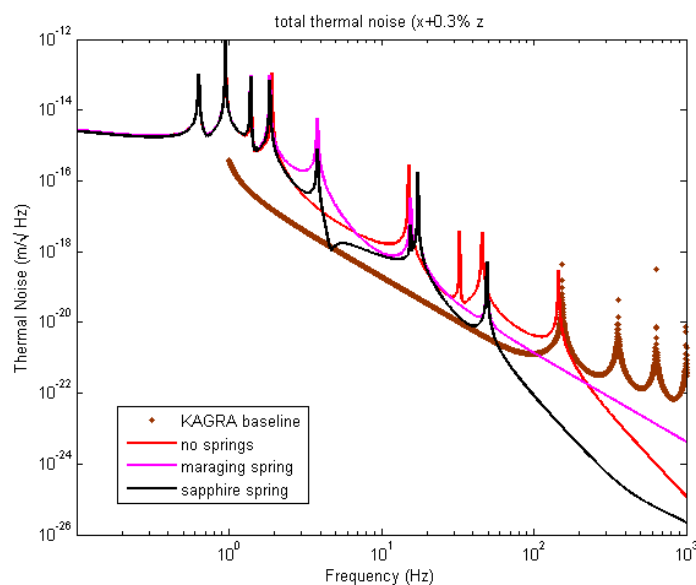


Figure 5. Thermal noise estimate with springs at the final stage (for a single test mass)

3. Sapphire Spring Strength Tester

Cantilever beam breaking tests have been undertaken on IMPEX sapphire slide samples provided by KAGRA, as shown in figure 6.

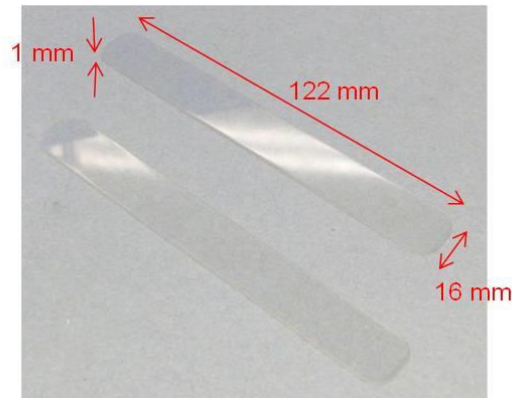


Figure 6. IMPEX sapphire slide

A cantilever bending strength test setup was used to break the slides by applying a force to their end and measuring the maximum deflection of the slide prior to failure. The apparatus is shown in Figure 7. Breaking occurs at the clamping point, with maximum stress:

$$\sigma = \frac{3Yt \cdot \text{deflection}}{2L^2}$$

where Y is the Young's modulus, t is the thickness and L is the length of slide exposed to bending.

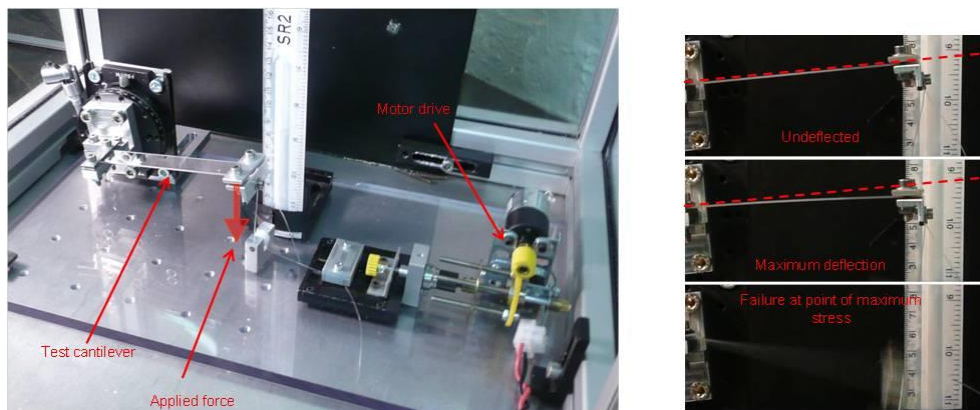


Figure 7. Cantilever spring strength testing apparatus

4. Sapphire Spring Tests

A total of 26 sapphire samples were tested. Of these, 8 were mechanically polished and 18 were thermo-polished, 2 of which failed to break. The results of the breaking stress are shown in figure 8.

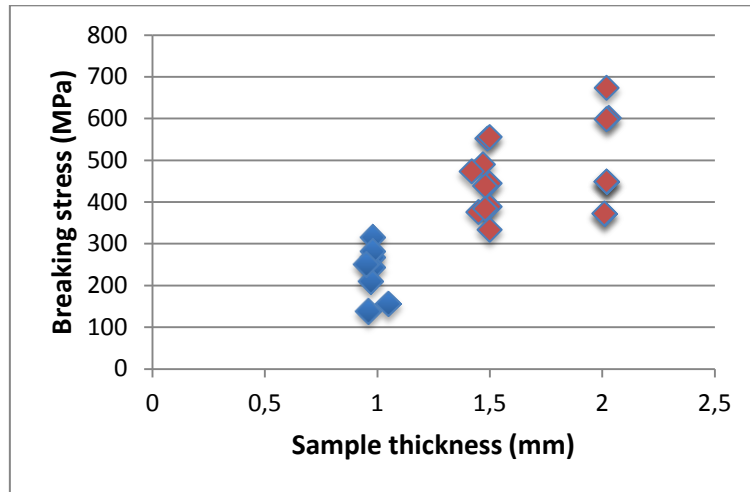


Figure 8. Breaking stress of sapphire slides at maximum deflection.

The mechanically polished slides, shown as blue data points, were all approximately 1mm thick and had a maximum breaking stress of 315.9MPa. The samples with a thermo-polished finish, shown as red data points, were a combination of 1.5 mm and 2 mm thick. These demonstrated a maximum breaking stress of 555.4 MPa and 598.1 MPa respectively. The two samples which failed to break had stresses of 673.2 MPa and 601.1 MPa at the maximum deflection point without failing.

It is therefore evident that the thermo-polished samples are stronger, taking into account the extra thickness. Work is now being undertaken on analyzing the surfaces of these slides in order to investigate how the finish contributes to the strength.

5. Sapphire fibre strength tests

Tensile strength tests have been undertaken on several sapphire samples supplied by KAGRA. These comprised of two tests (as shown in figure 9) – a ~3x overload mass hang and a destructive tensile strength test undertaken on a dedicated tensile strength testing machine previously used to test fibre and weld strengths for Advanced LIGO fibres [3]. Two fibre types were used – simple constant diameter (1.8 mm) fibre sections manufactured by Moltech; and fibres with nail ends manufactured by IMPEX, as shown in figure 10.

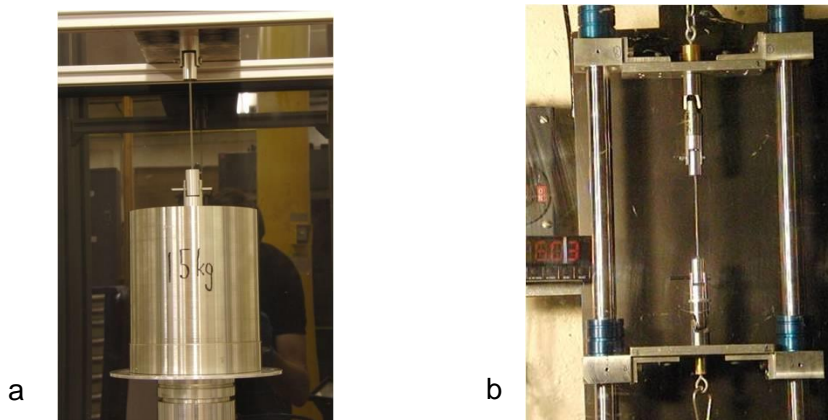


Figure 9a. Moltech fibre hanging 15 kg strength test mass b. Moltech fibre on tensile strength testing machine, at point of failure (in the clamp) at 60.3 kg.



Figure 10. IMPEX nail end fibre.

The Moltech fibre successfully suspended 4 kg, 10 kg and 15 kg strength test masses as shown in figure 9a. Four destructive strength tests were undertaken on the same fibre – no failure was observed in any of the cases – pull out of the clamps was observed at 24.5 kg, 40.2 kg, 60.1 kg and 60.3 kg. The maximum strength shown was over a factor 10x greater at 294 MPa than the suspension load per fibre of 22.2 MPa (5.75 kg) that will be experienced in the KAGRA suspension.

The jig for testing of nail end fibres is shown in figure 11. The IMPEX fibre was shown to have a tensile strength of 50.3 kg (194 MPa). Failure occurred at the interface between the nail end and the fibre. This strength is a comfortable factor of 8.7 greater than the suspension load (see figure 11b).

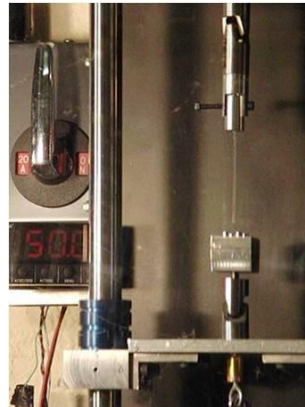
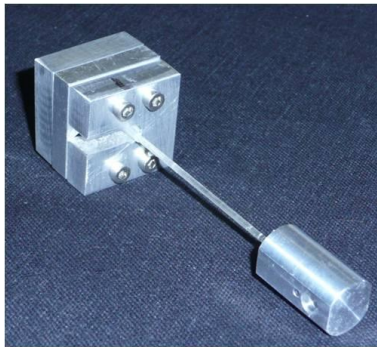
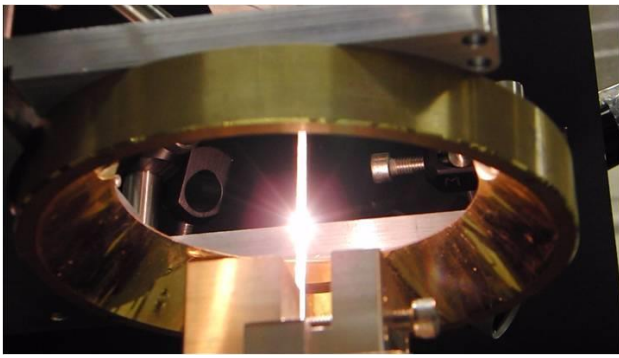


Figure 11a. IMPEX nail end fibre clamping jig b. IMPEX nail end fibre on tensile strength testing machine, just before point of failure (fracture at nail end) at 50.3 kg.

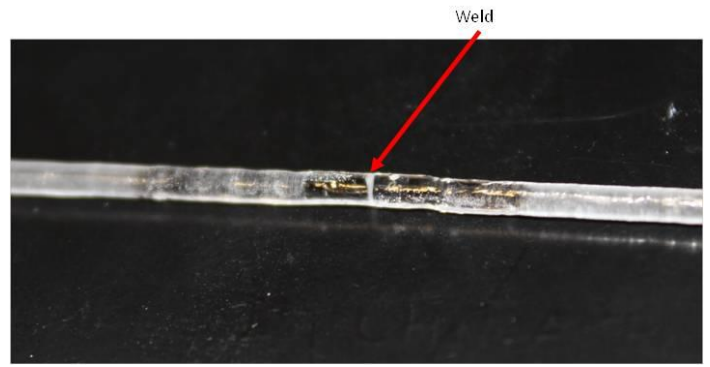
6. Sapphire laser weld tests

It is possible to heat sapphire to melting with CO₂ laser, so tests were undertaken on broken pieces of the fibres strength tested in section 5 to see if re-joining was possible. This may provide another possible method of suspension construction.

Figure 12a shows two pieces of sapphire fibre being heated using a conical mirror arrangement within Glasgow's laser pulling machine [4]. The two pieces of fibre had their ends butted together and this point was heated with up to 100 W of CO₂ laser power. No significant pressure was applied to the joint along the axis of the fibre and the parts were seen to join easily to re-form a single piece of sapphire fibre, as shown in Figure 12b.

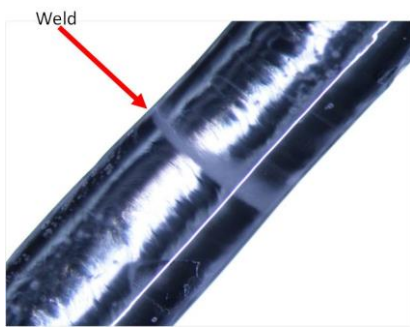


a.

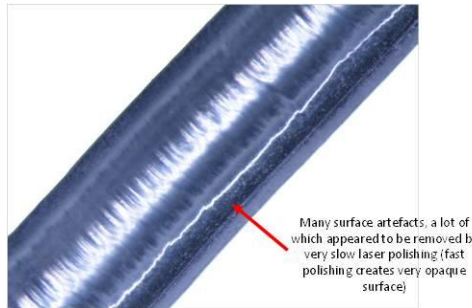


b.

Figure 12a. Heating of sapphire with CO₂ laser, b Welded piece of sapphire showing 'weld' point.



a.



b.



c.

Figure 13a. Welded piece of sapphire showing 'weld' point under microscope, b Microscope image of untouched opaque region of Moltech fibre c. Microscope image of laser polished region of Moltech fibre showing less small scale surface artefacts.

The weld was seen to have a visible join line but smooth surfaces were seen over the join region. It was also observed during this process that the surface quality of the samples appeared to have been improved by the laser heating – fewer surface artefacts were observed after heating, seen in the microscope images shown in figure 13, and the surface changed from being opaque to transparent. This provides an interesting possibility for improving the surface quality, and possibly the surface dissipation of the sapphire fibres and is an interesting area in which further research could be undertaken. Currently research is ongoing into methods of production of fibres via heating with the CO₂ laser and drawing a crystalline fibre from the molten region (laser heated pedestal growth).

7. References:

- [1] <http://www.ligo.caltech.edu/~e2e/SUSmodels/>
- [2] ELiTES Dropbox (..\Dropbox\ELiTES WP2\material properties)
- [3] LIGO document T1000345, <https://dcc.ligo.org/LIGO-T1000345>
- [4] [Rev Sci Instrum.](#) 2011 Jan;82(1):011301. doi: 10.1063/1.3532770

Appendix A

Maraging steel	
Density (kg/m ³)	7800
Specific heat (J/kg K)	10
Thermal conductivity (W/mK)	2
Thermal expansion coefficient (1/K)	-8×10^{-7}
Young's modulus (GPa)	187
Young's modulus change with temperature: $1/Y dY/dT$ (1/K)	0
Bulk damping	10^{-4}
Surface damping	0
Tungsten	
Density (kg/m ³)	19100
Specific heat (J/kg K)	6
Thermal conductivity (W/mK)	1000
Thermal expansion coefficient (1/K)	-8×10^{-7}
Young's modulus (GPa)	400
Young's modulus change with temperature: $1/Y dY/dT$ (1/K)	0
Bulk damping	10^{-4}
Surface damping	0
Sapphire	
Density (kg/m ³)	4000
Specific heat (J/kg K)	0.716
Thermal conductivity (W/mK)	575
Thermal expansion coefficient (1/K)	4×10^{-9}
Young's modulus (GPa)	400
Young's modulus change with temperature: $1/Y dY/dT$ (1/K)	0
Bulk damping	7×10^{-10}
Surface damping	6×10^{-10}

Table A1. Thermo-mechanical and damping parameters